THE JOURNAL OF PHYSICAL CHEMISTRY C

ARTICLE

pubs.acs.org/JPCC

Preventing Graphene Sheets from Restacking for High-Capacitance Performance

Yan Wang, Yingpeng Wu, Yi Huang, Fan Zhang, Xi Yang, Yanfeng Ma, and Yongsheng Chen*

Key Laboratory of Functional Polymer Materials and Center for Nanoscale Science and Technology, Institute of Polymer Chemistry, College of Chemistry, Nankai University, Weijin Road 94, Tianjin 300071, China

ABSTRACT: Aiming at preventing restacking of individual graphene sheets by using a simple green hydrothermal route, we have introduced carbon nanotubes to act as the spacer in fabricating a three-dimensional (3-D) hierarchical structure with graphene sheets. These 3-D hierarchical structure materials have been used to fabricate supercapacitor devices, and a high specific capacitance of 318 F/g for graphene with an energy density of 11.1 (W h)/kg has been achieved.

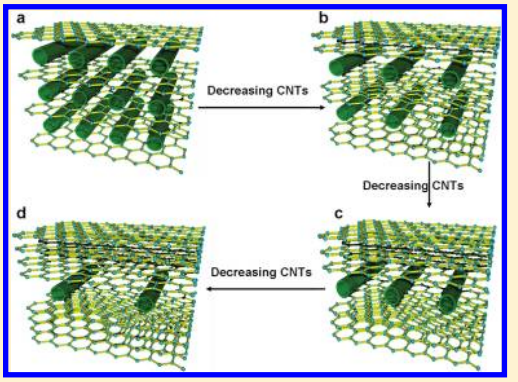

1. INTRODUCTION

Owing to their unique high conductivity and large specific surface area,[1,2] graphene nanosheets are expected to be an ideal material for energy storage and conversion.[3−8] The theoretical specific surface area for completely exfoliated and isolated graphene sheets is ∼2600 m^2/g and can provide a specific capacitance of about 550 F/g, according to the intrinsic capacitance of graphene (21 μF/cm^2) reported recently.[3−5] However, the restacking of graphene sheets has hampered the performance of supercapacitors using graphene materials.[7,8] The success of materializing graphene's high surface area and conductivity, thus for a high-performance supercapacitor with graphene, depends on the fabrication process of active materials and electrodes to avoid such restacking.[7,8] In the past few years, many works using graphene as the active electrode material for supercapacitors have been reported, and these works can be roughly cataloged into two types. The first one uses only the graphene-based materials as the active materials without adding any other electroactive materials. The graphene materials used in this catalog can be "pristine" graphene,[9] graphene oxide (GO), or activated GO.[10−14] Most such graphene materials start from GO, including the reduced GO materials prepared by hydrazine reduction,[3,4] hydrothermal treatment,[15,16] microwaves,[17] vacuum-promoted exfoliation,[18] and chemical activation of exfoliated graphite oxide.[11,13,19] The reported specific capacitance for aqueous systems is in the range of 90−264 F/g from these works. There are also some reports on graphene-based supercapacitors using organic electrolyte systems.[5,20,21] Obviously, these approaches so far have had limited success, corresponding to the theoretical capacitance of 550 F/g for graphene.[5] The key issue using this approach is preventing the restacking and agglomeration of graphene sheets during the electrode fabrication process,[4,22] as the restacking of graphene sheets will diminish the super high surface area of graphene to close to that (∼10 m^2/g) of graphite and probably reduce the bulky conductivity of the materials too.[23]

In addition to carbon-based materials, metal oxides and conducting polymers have been widely studied as the active materials in supercapacitors. Therefore, the second approach using graphene for supercapacitors is to combine it with other metal oxides or conductin7g polymers to form graphene hybrid materials,[24−26] mainly to use their pseudocapacitance.[22,27,28] This has been carried out by quite a few groups with a wide range of materials and performances (e.g., specific capacitance from hundreds to >1000 F/g). Polyaniline (PANI)[29−35] is mostly studied among conducting polymers.[25,26,29] Different metal oxides with graphene using MnO_2,[36−38] Fe_3O_4,[39] NiO,[40] and RuO_2[22] have also been reported. Similarly, other carbon materials, such as activated carbon or carbon nanotubes, could also be used for the same purpose, though no extra pseudocapacitance such as that from metal oxides or conducting polymers could be offered.[22,27,28,41] For example, nanosized and functionalized carbon black particles have been attached onto the surface of the graphene sheets and serve as spacers to separate and support the neighboring sheets.[27] Wei et al. reported a method[28] to prepare a graphene/carbon nanotube (CNT) hybrid using chemical vapor deposition (CVD) in situ growth, and its supercapacitor performance has been studied. A film made from a direct GO/multiwalled CNT mixture has been used for supercapacitors and possesses a specific capacitance of 265 F/g at 100 mA/g.[42]

Received: July 8, 2011
Revised: August 7, 2011
Published: October 13, 2011

Table 1. Composition of GO/CNT Solutions[a]

sample	amt of GO solution (mL)	amt of CNT solution (mL)	GO:CNT ratio
1	0	70	0:1
2	35	35	1:1
3	46.7	23.3	2:1
4	56	14	4:1
5	60	10	6:1
6	62.2	7.8	8:1
7	63.6	6.4	10:1
8	70	0	1:0

[a] All samples were made from GO and CNT solutions with a concentration of 2 mg/mL to yield a total of 70 mL of solution.

With so many reports on graphene for supercapacitor application, it should be noted that the measurements and calculation methods are not all the same even for the same materials, or with the same error ranges, so the results may not be compared directly in some cases.

Obviously, one of the best strategies to materialize the great potential of graphene for supercapacitors is to add some spacer between the graphene sheets to avoid such restacking and agglomerate formation, and in the meantime, the spacer could best contribute to the active material's overall surface area and/or conductivity. In this work, taking advantage of the high conductivity and nanoscale size of CNTs, we designed and fabricated a three-dimensional (3-D) hierarchical structure of graphene using CNTs as the spacer between the graphene sheets via a simple yet green hydrothermal route. These 3-D hierarchical structure materials were then used to fabricate supercapacitor devices as the electrode active materials, and a high specific capacitance of 318 F/g of graphene with an energy density of 11.1 (W h)/kg was achieved. These results demonstrate that the spacing strategy would offer an easy and effective way to fabricate supercapacitors using graphene, which could be applied as a general approach for other materials.

2. EXPERIMENTAL SECTION

2.1. Materials. GO was prepared by oxidation of natural graphite powder (average particle size of 20 μm, Qingdao Huarun Graphite Co., Ltd.) with the modified Hummers method, as we described elsewhere.[43] The as-prepared GO solution (2 mg/mL) was prepared as a stable aqueous dispersion using ultrasonication.[43] For CNTs, we used multiwalled carbon nanotubes (TNMC3, −COOH content 2 wt %, Chengdu Organic Chemicals Co. Ltd.). Thus, 200 mg of CNTs was added to a pre-prepared sodium dodecylbenzenesulfonate (SDBS) water solution (100 mL, 10 mg/mL) and then treated with ultrasonication for 2 h to obtain the CNT solution. Poly(tetrafluoroethylene) (PTFE) binder was purchased from China Chenguang Co., Ltd.. The polypropylene film was purchased from China Siteng Co., Ltd. as the separator.

2.2. Preparation of GO/CNT Solutions. A series of GO/CNT solutions with different weight ratios of GO to CNTs have been made according to Table 1. The GO/CNT solutions were prepared from the two solutions of GO (2 mg/mL) and CNTs (2 mg/mL) above with the desired amounts and then sonicated for 2 h.

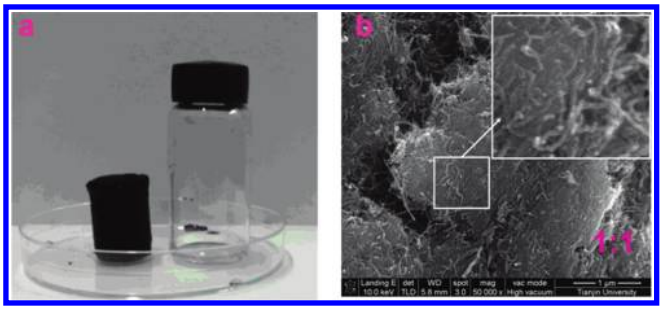

Figure 1. (a) Optical image of the G/CNT hydrogel hybrid. (b) A typical SEM image for a G:CNT ratio of 1:1. The inset shows the enlarged scale.

2.3. Hydrothermal Treatment of GO/CNT Solutions. All the solutions listed in Table 1 were transferred to a sealed 100 mL Teflon-lined autoclave, heated to 180 °C, and then maintained at for 18 h. The autoclave was then cooled to room temperature. A hydrogel material of graphene (G)/CNTs was obtained from this process, which was then taken out and blotted with a filter paper to remove surface-adsorbed water for the following experiments. The as-prepared hydrogels were thoroughly washed with water to remove the surfactant SDBS. The products of G/CNTs were finally dried for 24 h at 120 °C in vacuum to completely remove water solvent.

2.4. Fabrication of Supercapacitors with the G/CNT Hybrid. The industry-level supercapacitor cells (coin style) were fabricated with the two-electrode configuration. The two electrodes were made of the G/CNT hybrid materials listed in Table 1, mixed with 10 wt % PTFE binder, and then fabricated with a thin polypropylene film as the separator. A 30 wt % KOH aqueous solution was used as the electrolyte. The mixture of 3-D hybrid and PTFE was homogenized in water by being sonicated for 30 min and then dried for 24 h in a vacuum oven at 120 °C to completely remove water. The electrodes, which were pressed on a Ni foam current collecting electrode (∅ = 13 mm) with a pressure of 20 MPa, were separated by the polypropylene film and were sandwiched in a stainless steel cell with a pressure of 160 MPa.[4]

2.5. Electrochemical Measurements. The electrochemical properties and capacitance measurements of supercapacitor electrodes were studied in a two-electrode system by galvanostatic charge−discharge with a supercapaicitor tester (Arbin Instruments). Testing was carried out at potentials between 0 and 1.0 V using 30 wt % KOH aqueous electrolyte.

2.6. Characterization. Scanning electron microscopy (SEM) was performed on a LEO 1530VP field emission scanning electron microscope with an acceleration voltage of 10 kV. N_2 adsorption−desorption analysis was done at 77 K on a Micromeritics ASAP 2020 apparatus.

3. RESULTS AND DISCUSSION

As mentioned above, to realize the full potential of graphene for supercapacitors, one key is to materialize its entire theoretical surface area and conductivity, so a solution process of GO and CNTs in homogeneously distributed water solutions of these two materials was used to achieve the best dispersion of both the graphene sheet and CNTs.[15,16,44] During the following hydrothermal process, several things could happen to functional groups such as COOH and OH on both graphene sheets and

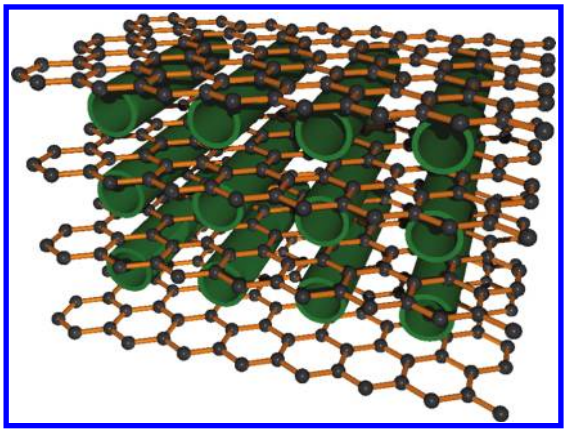

Figure 2. Model for an ideal state of the 3-D hybrid graphene/CNTs.

CNTs. First, these functional groups could be lost, and thus, the intrinsic π structure and conductivity of graphene and CNTs could be recovered.[15,16,45] Simultaneously, these oxygenated functional groups on the graphene sheets and CNTs could react and bond together. These actions, together with the reduced hydrophilicity of graphene and CNTs due to the removal of the oxygenated functional groups under hydrothermal conditions, could cause the graphene sheets and CNTs to form a 3-D hierarchical structure that appears visibly, as the hydrogel materials shown in Figure 1a.[15,16] It has been reported that GO could form such a 3-D structure quite easily with different materials containing various groups such as OH as just in water.[16,45] Also, as a control experiment, treatment of CNT solution could not produce such a hydrogel material. As can be seen from a typical SEM image (Figure 1b) for a G/CNT (ratio 1:1) gel material, graphene and CNTs have formed a homogeneous and 3-D structure. Stable hydrogel materials and similar SEM images could be obtained for different graphene and CNT ratios from 1:1 to 2:1, 4:1, 6:1, 8:1, and 10:1, but when the amount of GO is too low, such as when the G:CNT ratio is 1:2, no such hydrogel material could be obtained. This is similar as that observed in other literature.[16,45]

The ability of GO to form 3-D structures through a hydrothermal process has been intensively investigated recently by Shi[15,16] and other groups.[46] It should be noted that an initial H-bonding interaction between the OH and COOH groups on both graphene and CNTs should exist at the initial mixed state in their water solutions. Then, during the hydrothermal process, further chemical bonding in situ between these groups could anchor the initial homogeneous distribution of graphene sheets and CNTs and simultaneously remove most of the functional groups and defects on the graphene sheets. This process thus could form the expected 3-D hierarchical structure, with increased conductivity of graphene and CNTs. An *ideal* state of such a 3-D structure is shown in Figure 2, where graphene sheets are separated completely by CNTs in the state of individual layers. Thus, due to the existence of CNTs in this 3-D hierarchical structure, graphene sheets could be kept completely from restacking if the initial homogeneous distribution of CNTs and graphene sheets is completely kept. It should be noted that, in this ideal state, the entire surface of graphene could be exposed, and the electrolyte ions would also use the channels generated by the CNT spacer and thus facilitate the charging/recharging process of the devices.[47−50]

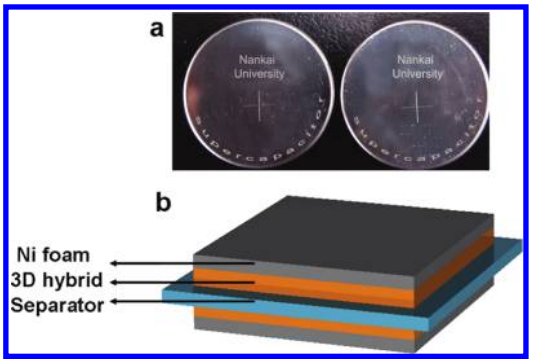

Figure 3. (a) Optical image of the coin-cell supercapacitor assembled according to the industry procedure. (b) Schematic diagram of the supercapacitor based on the 3-D G/CNT hybrid.

Table 2. Supercapacitor Performance Using the G/CNT Hybrid as the Active Electrode Material with Different Weight Ratios[a]

G:CNT ratio	C_I, F/g	E_I, (W h)/kg	C_G, F/g	E_G, (W h)/kg	BET SSA, m^2/g
0:1	9	0.3			200
1:1	112	3.9	318	11.1	237
2:1	129	4.5	249	8.6	278
4:1	143	5.0	210	7.3	305
6:1	164	5.7	216	7.5	356
8:1	181	6.6	224	7.8	397
10:1	187	6.5	223	7.7	407
1:0	190	6.6	190	6.6	374

[a] C_I is the integrated specific capacitance based on the overall weight of the graphene and CNTs, E_I is the energy density based on all the weight of both graphene and CNTs, C_G and E_G are the calculated effective specific capacitance and energy density of the graphene, respectively, and SSA is the specific surface area of the 3-D hybrids.

Using these hybrid materials, the coin-cell styles of supercapacitor devices were fabricated following the standard industry procedure as shown in Figure 3. The performance of the supercapacitor devices using these hybrid materials was studied in a two-electrode system by galvanostatic charge−discharge at a constant current density of 100 mA/g with a supercapacitor tester (Arbin Instruments). The specific capacitance is calculated from the slope of the charge−discharge curves according to the equation $C = I\Delta t/(m\Delta V)$, where I is the applied current and m is the total mass of each electrode.[8,51] The detailed fabrication is described in the Experimental Section, and the supercapacitor testing results of these industry-level devices are summarized in Table 2, where C_I is the integrated specific capacitance based on the *overall* weight of the graphene and CNTs, E is the energy density (E_I) based on *all* the weight of both graphene and CNTs, and C_G and E_G are the calculated effective and specific capacitance and energy density of the graphene, respectively. The energy densities E_I and E_G are calculated with $CV_i^2/2$, where C is the cell capacitance (one-quarter of the specific capacitances C_I and C_G) and V_i is the initial voltage (1.0 V).[47] The specific surface area (SSA) of the 3-D hybrids was measured with the N_2 adsorption Brunauer−Emmett−Teller (BET) method.

For comparison, we have first tested the supercapacitor performance using just graphene and CNTs under the same

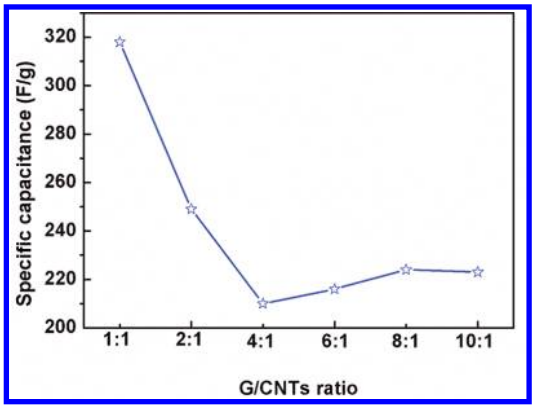

Figure 4. Effective specific capacitance of graphene in the hybrid materials with different ratios of G to CNTs.

conditions and procedures, which gives specific capacitances of 9 and 190 F/g for CNTs and GO, respectively. Note that the specific capacitance for the control supercapacitor using CNTs gave no significant capacitance (9 F/g). It should be noted that the overall specific capacitance (C_I) of the G/CNT hybrid materials should be considered as the total contribution of graphene and CNT together. To get the effective specific capacitance of graphene for the hybrid materials with different G:CNT ratios, we use the following equation:

$$C_I(R \times 0.48 + 1 \times 0.96) = C_G(R \times 0.48) + C_C \times 1 \times 0.96 \quad (1)$$

where C_I is the overall experimental specific capacitance of the hybrid materials based on the effective total mass of graphene and CNTs, R is the initial weight ratio of G to CNTs (for ratios of 1:1, 2:1, 4:1, 6:1, 8:1, and 10:1, R = 1, 2, 4, 6, 8, and 10, respectively), C_G is the effective specific capacitance of graphene, and C_C is the specific capacitance of CNTs. From the control experiments, the remaining effective weight percentages of GO and CNTs during the hydrothermal process are 48% and 96%, respectively, so these factors are applied in the calculation using eq 1. Note that, due to the rather low specific capacitance of CNTs (9 F/g) and no significant capacitance change expected for CNTs during the hydrothermal treatment together with GO,[42] we could use eq 1 to calculate the effective specific capacitance of graphene in the hybrid materials for the different ratios (1:1, 2:1, 4:1, 6:1, 8:1, 10:1), which are represented in Table 2.

The effective specific capacitance of graphene in the different hybrid materials is plotted in Figure 4 for better understanding. First, the best performance of graphene is from the G/CNT hybrid with a ratio of 1:1, which gives a record high 318 F/g capacitance, 64% of the value of graphene in theory.[5] This is significantly higher than that (190 F/g) from just graphene in our control experiment. Unfortunately, we could not get results which would be better for the hybrids with more CNTs under the same hydrothermal procedure, since no solid hydrogel 3-D materials could be obtained at the time. As shown in Figure 4, all of the specific capacitances of graphene in the hybrid materials are higher than that obtained from just using graphene (190 F/g). Furthermore, with decreasing CNT loading, the effective capacitance first decreases but approaches a steady value later. These results indicate that the addition of CNTs could indeed enhance the specific capacitance of graphene by preventing its restacking as we discussed earlier.

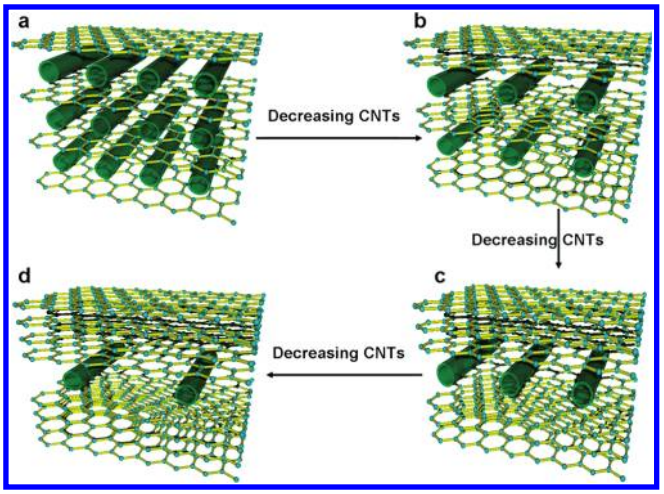

Figure 5. Schematic diagram of 3-D hybrid structure engineering with decreasing spacer CNT loading (from a to d).

To help understand the change of these specific capacitance results, we have drawn a scheme in Figure 5 to clarify our understanding. First, when only GO was treated in the hydrothermal process, some of the graphene sheets unavoidably restacked together as observed in many earlier works.[6−8] When CNTs were added and mixed homogeneously with graphene sheets, the 3-D hierarchical structures of graphene sheets with CNTs formed in situ and the homogeneous state could be "frozen" in the following hydrothermal process. With decreasing amounts of CNTs as shown in Figure 5 (from a to d), the restacking of the graphene sheets would increase due to less CNT spacing.

As we can observe from Figure 4, with the ratio of G to CNTs increasing, the effective specific capacitance of graphene decreases and then approaches a steady value. On the basis of the scheme shown in Figure 5, we can see that when the ratio of G to CNTs increases such as from part a to part d of Figure 5, the restacking of graphene will be serious. This could have an influence on the effective surface area of the graphene material, and thus the effective contribution of graphene to the overall capacitance of the entire electrode active material (G/CNT hybrid) would decrease. This is expected to make the effective specific capacitance of graphene smaller as we observed in Table 2 and Figure 4. Therefore, the loading ratio of CNTs could engineer the hybrid structure and the overall capacitance of the graphene.[8,47,51]

Galvanostatic cycling of supercapacitor electrodes was performed at different constant current densities of 100, 250, 500, and 1000 mA/g. As seen in Figure 6 for the hybrid with a G:CNT ratio of 10:1, the discharge curves are linear in the total range of potential with constant slopes, showing nearly perfect capacitive behavior.[47,48] The specific capacitances are 187, 181, 170, and 167 F/g at the corresponding current density. These data show that the specific capacitance of 3-D hybrid G/CNTs (10:1) hold ~90% of their specific capacitance at the high current density (Figure 6b), suggesting good rate capability.[5,47,48] For this 3-D hybrid structure, the space between graphene sheets was kept and the resistance of the graphene sheet was lowered by the connected CNTs, which facilitate the electrolyte ions to move quickly at a high current density and exhibits good rate performance.

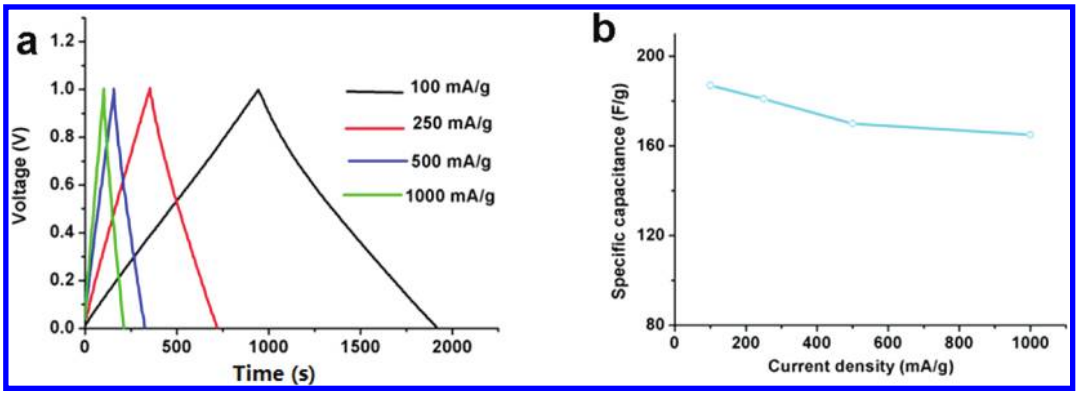

Figure 6. (a) Galvanostatic charge−discharge curve of the supercapacitor using G/CNTs (10:1) as the active material at constant current densities of 100, 250, 500, and 1000 mA/g using 30 wt % KOH electrolyte. (b) Specific capacitance of 3-D hybrid G/CNTs (10:1) measured at different current densities.

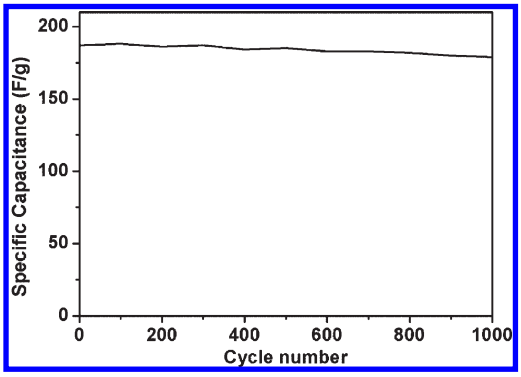

Figure 7. Change of the specific capacitance of 3-D hybrid G/CNTs (10:1) as a function of the cycle number at a constant current density of 100 mA/g.

A long cycle life of a supercapacitor is important for its practical applications. Figure 7 shows the variation of specific capacitance with cycle number for the G/CNT (10:1) supercapacitor at a constant current density of 100 mA/g. Cycle lives in excess of 1000 cycles have been tested. As can be seen, the specific capacitance still remains at 179 F/g (∼95%) after 1000 cycles of testing.

From these results, we can see that using CNTs as the spacer to prevent the restacking of graphene sheets could indeed improve the performance of graphene in a supercapacitor and that this strategy could be applied to other materials and devices.

4. CONCLUSION

In summary, homogeneously distributed graphene/CNT 3-D hybrids have been fabricated by a simple and green hydrothermal route. The addition of the CNTs could engineer the stacking of graphene sheets and keep the space between the neighboring graphene sheets, thus enhancing its effective surface area and performance in a supercapacitor. The 3-D hybrid gave the best result with a specific capacitance of 318 F/g for graphene. This green and simple strategy could also be used for materials other than graphene and improve the overall supercapacitor performance.

■ ACKNOWLEDGMENT

The authors gratefully acknowledge financial support from the MOST (Grants 2012CB933401 and 2011DFB50300), NSFC (Grants 50933003, and 50903044).

■ REFERENCES

(1) Geim, A. K. *Science* **2009**, *324*, 1530.
(2) Geim, A. K.; Novoselov, K. S. *Nat. Mater.* **2007**, *6*, 183.
(3) Stoller, M. D.; Park, S. J.; Zhu, Y. W.; An, J. H.; Ruoff, R. S. *Nano Lett.* **2008**, *8*, 3498–3502.
(4) Wang, Y.; Shi, Z. Q.; Huang, Y.; Ma, Y. F.; Wang, C. Y.; Chen, M. M.; Chen, Y. S. *J. Phys. Chem. C* **2009**, *113*, 13103.
(5) Liu, C. G.; Yu, Z. N.; Neff, D.; Zhamu, A.; Jang, B. Z. G. *Nano Lett.* **2010**, *10* (12), 4863.
(6) Xia, J. L.; Chen, F.; Li, J. H.; Tao, N. J. *Nat. Nanotechnol.* **2009**, *4*, 505.
(7) Zhang, L. L.; Zhou, R.; Zhao, X. S. *J. Mater. Chem.* **2010**, *20*, 5983.
(8) Brownson, D.; Kampouris, D.; Banks, C. *J. Power Sources* **2011**, *196*, 4873.
(9) Zhang, K.; Mao, L.; Zhang, L.; Chan, H.; Zhao, X. S.; Wu, J. S. *J. Mater. Chem.* **2011**, *21*, 7302.
(10) Yu, A. P.; Roes, I.; Davies, A.; Chen, Z. W. *Appl. Phys. Lett.* **2010**, *96*, 253105.
(11) Li, Y.; van Zijll, M.; Chiang, S.; Pan, N. *J. Power Sources* **2011**, *196*, 6003.
(12) Du, Q. L.; Zheng, M. B.; Zhang, L. F.; Wang, Y. W.; Chen, J. H.; Xue, L. P.; Dai, W. J.; Ji, G. B.; Cao., J. M. *Electrochim. Acta* **2010**, *55*, 3897.
(13) Le, L. T.; Ervin, M. H.; Qiu, H. W.; Fuchs, B. E.; Lee, W. Y. *Electrochem. Commun.* **2011**, *13*, 355.
(14) Yoo, J. J.; Balakrishnan, K.; Huang, J. S.; Meunier, V.; Sumpter, B. G.; Srivastava, A.; Conway, M.; Reddy, A. L. M.; Yu, J.; Vajtai, R.; Ajayan, P. M. *Nano Lett.* **2011**, *11*, 1423.
(15) Sheng, K. X.; Xu, Y. X.; Li, C.; Shi, G. Q. *New Carbon Mater.* **2011**, *26*, 9.
(16) Xu, Y. X.; Sheng, K. X.; Li, C.; Shi, G. Q. *ACS Nano* **2010**, *4*, 4324.
(17) Chen, Y. M.; Yan, L. F.; Bangal, P. *Carbon* **2010**, *48*, 1146.
(18) Lv, W.; Tang, D. M.; He, Y. B.; You, C. H.; Shi, Z. Q.; Chen, X. C.; Chen, C. M.; Hou, P. X.; Liu, C.; Yang, Q. H. *ACS Nano* **2009**, *3*, 3730.
(19) Zhu, Y. W.; Shanthi, M.; Stoller, M. D.; Ruoff, R. S. *Science* **2011**, *332*, 1537.
(20) Hantel, M. M.; Kaspar, T.; Nesper, R.; Wokaun, A.; Kotz, R. *Electrochem. Commun.* **2011**, *13*, 90.
(21) Kim, T. Y.; Lee, H. W.; Stoller, M.; Dreyer, D. R.; Bielawski, C. W.; Ruoff, R. S.; Suh, K. S. *ACS Nano* **2011**, *5*, 436.
(22) Wu, Z. S.; Wang, D. W.; Ren, W.; Zhao, J.; Zhou, G.; Li, F.; Cheng, H. M. *Adv. Funct. Mater.* **2010**, *20*, 3595.
(23) Wang, X; Zhi, L.; Mullen, K. *Nano Lett.* **2008**, *8*, 323.
(24) Chen, S.; Zhu, J. W.; Wang, X. *ACS Nano* **2010**, *4*, 6212.
(25) Zhang, L. L.; Zhao, S. Y.; Tian, X. N.; Zhao, X. S. *Langmuir* **2010**, *26*, 17624.

(26) Zhang, K.; Ang, B. T.; Zhang, L. L.; Zhao, X. S.; Wu, J. S. *J. Mater. Chem.* **2011**, *21*, 2663.
(27) Yan, J.; Wei, T.; Shao, B.; Ma, F. Q.; Fan, Z. J.; Zhang, M. L.; Zheng, C.; Shang, Y. C.; Qian, W. Z.; Wei, F. *Carbon* **2010**, *48*, 1731.
(28) Fan, Z. J.; Yan, J.; Zhi, L. J.; Zhang, Q.; Wei, T.; Feng, J.; Zhang, M. L.; Qian, W. Z.; Wei, F. *Adv. Mater.* **2010**, *22*, 3723.
(29) Hao, Q. L.; Wang, H. L.; Yang, X. J.; Lu, L. D.; Wang, X. *Nano. Res.* **2011**, *4*, 323.
(30) Mini, P. A.; Balakrishnan, A.; Nair, S. V.; Subramanian, K. R. V. *Chem. Commun.* **2011**, *47*, 5753.
(31) Zhang, K.; Zhang, L. L.; Zhao, X. S.; Wu, J. S. *Chem. Mater.* **2010**, *22*, 1392.
(32) Yan, J.; Wei, T.; Fan, Z. J.; Qian, W. Z.; Zhang, M. L.; Shen, X. D.; Wei, F. *J. Power Sources* **2010**, *195*, 3041.
(33) Wang, H. L.; Hao, Q. L.; Yang, X. J.; Lu, L. D.; Wang, X. *ACS Appl. Mater. Interfaces* **2010**, *2*, 821.
(34) Wu, Q.; Xu, Y. X.; Yao, Z. Y.; Liu, A. R.; Shi, G. Q. *ACS Nano* **2010**, *4*, 1963.
(35) Wang, D. W.; Li, F.; Zhao, J. P.; Ren, W. C.; Chen, Z. G.; Tan, J.; Wu, Z. S.; Gentle, I; Lu, G. Q.; Cheng, H. M. *ACS Nano* **2009**, *3*, 1745.
(36) Zhang, J. T.; Jiang, J. W.; Zhao, X. S. *J. Phys. Chem. C* **2011**, *115*, 6448.
(37) Cheng, Q.; Tang, J.; Ma, J.; Zhang, H.; Shinya, N.; Qin, L. C. *Carbon* **2011**, *49*, 2917.
(38) Yan, J.; Fan, Z. J.; Wei, T.; Qian, W. Z.; Zhang, M. L.; Wei, F. *Carbon* **2010**, *48*, 3825.
(39) Shi, W. H.; Zhu, J. X.; Sim, D. H.; Tay, Y. Y.; Lu, Z. Y.; Zhang, X. J.; Sharma, Y.; Srinivasan, M.; Zhang, H.; Hng, H. H.; Yan, Q. Y. *J. Mater. Chem.* **2011**, *21*, 3422.
(40) Wang, H. L.; Casalongue, H. S.; Liang, Y. Y.; Dai, H. J. *J. Am. Chem. Soc.* **2010**, *132*, 7472.
(41) Yu, D. S.; Dai, L. M. *J. Phys. Chem. Lett.* **2010**, *1*, 467.
(42) Lu, X.; Dou, H.; Gao, B.; Yuan, C.; Yang, S.; Hao, L.; Shen, L.; Zhang, X. *Electrochim. Acta* **2011**, *56*, 5115.
(43) Becerril, H. A.; Mao, J.; Liu, Z.; Stoltenberg, R. M.; Bao, Z.; Chen, Y. *ACS Nano* **2008**, *2*, 463.
(44) Yu, D. S.; Dai, L. M. *J. Phys. Chem. Lett.* **2010**, *1*, 467–470.
(45) Zhou, Y.; Bao, Q. L.; Tang, L. A. L.; Zhong, Y. L.; Loh, K. P. *Chem. Mater.* **2009**, *21*, 2950.
(46) Dubin, S.; Gilje, S.; Wang, K.; Tung, V. C.; Cha, K.; Hall, A. S.; Farrar, J.; Varshneya, R.; Yang, Y.; Kaner, R. B. *ACS Nano* **2010**, *4*, 3845.
(47) Conway, B. E. *Electrochemical Supercapacitors: Scientific Fundamentals and Technological Applications*; Kluwer Academic/Plenum Publishers: New York, 1999; Chapter 15.
(48) Burke, A. *J. Power Sources* **2000**, *91*, 37.
(49) Kotz, R.; Carlen, M. *Electrochim. Acta* **2000**, *45*, 2483.
(50) Winter, M.; Brodd, R. J. *Chem. Rev.* **2004**, *104*, 4245.
(51) Pandolfo, A. G.; Hollenkamp, A. F. *J. Power Sources* **2006**, *157*, 11.